J. Phys. B: At. Mol. Opt. Phys. **33** (2000) 4849–4861. Printed in the UK PII: S0953-4075(00)51241-3

Dissociative recombination of NO^+: calculations and comparison with experiment

I F Schneider†‡§, I Rabadán†‖, L Carata‡§, L H Andersen¶, A Suzor-Weiner‡+ and J Tennyson†

† Department of Physics and Astronomy, University College London, Gower Street, London WC1E 6BT, UK
‡ Laboratoire de Photophysique Moléculaire, Université Paris-Sud, F-91405 Orsay, France
§ National Institute for Lasers, Plasma and Radiation Physics, Bucharest-Măgurele, Romania
‖ Departamento de Química, Universidad Autónoma de Madrid, 28049-Madrid, Spain
¶ Institute of Physics and Astronomy, Aarhus University, DK-8000 Aarhus C, Denmark
+ Laboratoire de Chimie Physique, 11 rue Pierre et Marie Curie, F-75234 Paris, France

Received 6 July 2000, in final form 25 September 2000

Abstract. Multichannel quantum defect calculations for NO^+ dissociative recombination (DR) for electron energies from threshold to 8 eV are presented. The calculations use electronic energies and autoionization widths of valence states obtained from *ab initio R*-matrix calculations with the corresponding potential curves calibrated using available spectroscopic data. Six valence states open to dissociation are included in the final calculations. Excellent agreement with the measured cross sections is obtained for the low-energy DR, up to 3 eV and, for the first time, the peak observed in the cross section at high energy is accounted for. The importance of the various dissociative states at different electron energies, as well as the direct and indirect processes, is discussed. Compared to previous theoretical studies, the inclusion of a third dissociative state of $^2\Pi$ symmetry and the larger autoionization width of the $B'\,^2\Delta$ state are found to be particularly important for the agreement with experiment.

(Some figures in this article are in colour only in the electronic version; see `www.iop.org`)

1. Introduction

NO^+ is one of the most important ions in the terrestrial ionosphere, as well as in the thermosphere of Venus (Fox 1989, 1993), and its quenching is mainly due to dissociative recombination (DR):

$$NO^+ + e^- \rightarrow N + O. \tag{1.1}$$

The most recent experiments, using storage ring (Vejby-Christensen *et al* 1998) and flowing-afterglow-Langmuir-probe (Mostefaoui *et al* 1999) techniques, have measured a DR thermal rate of around 4×10^{-7} cm^3 s^{-1}, in good agreement with previous afterglow results (Dulaney *et al* 1987, Spanel *et al* 1993). It is for this ion that the first quantitative estimations of the DR thermal rate were performed (Bardsley 1968b) as an application of the configuration interaction method (Bardsley 1968a). The calculated value of 4.3×10^{-7} cm^3 s^{-1} confirmed the experimental results to date, and was close to a later result of 5×10^{-7} cm^3 s^{-1} obtained in the first attempt (Lee 1977) to model the DR process using the multichannel quantum defect theory (MQDT). A consistent MQDT-type approach to DR was elaborated only a few years later (Giusti-Suzor 1980), and new molecular data have been produced in the following decade

0953-4075/00/214849+13$30.00

(Raoult 1987, Nakashima *et al* 1989). However, surprisingly, the most recent calculations (Sun and Nakamura 1990, Vâlcu *et al* 1998) based on this method and data resulted in significantly smaller thermal rates than the experimental ones, i.e. 1.7 and 0.9×10^{-7} cm^3 s^{-1}, respectively.

The high-energy region has been explored by merged-beam experiments. Single-pass measurements determined cross sections for incident electron energies up to 4 eV (Walls and Dunn 1974, Mul and McGowan 1979). The only theoretical cross section available in this region (Sun and Nakamura 1990) is smaller than the measured ones, the disagreement increasing with energy up to one order of magnitude at 2 eV. The most interesting high-energy feature was revealed by the multipass (storage-ring) experiment performed in Aarhus (Vejby-Christensen *et al* 1998): it is a broad maximum around 5 eV, similar to the giant 'resonances' found in the storage-ring measurements on H_2^+ and isotopomers (Forck *et al* 1993, Strömholm *et al* 1995, Tanabe *et al* 1995, Schmidt *et al* 1996, Andersen *et al* 1997) and H_3^+ and its isotopomers (Larsson *et al* 1993, Tanabe *et al* 2000). No firm theoretical explanation—qualitative or quantitative—has up to now been given for this feature in NO^+. Recently, a series of *ab initio* calculations of the NO states relevant to DR (and of the couplings between them) has been performed by Rabadán and Tennyson (1996, 1997, 1998) using the *R*-matrix method (Tennyson 2000). The data obtained made possible a new MQDT investigation of the process over the whole energy range explored by the experiments. To explain the broad peak at high energy (Vejby-Christensen *et al* 1998) and to re-evaluate the thermal rate using these data are the main goals of this paper.

2. The MQDT-type approach to DR

The extension of the MQDT approach (Seaton 1983, Greene and Jungen 1985) to dissociative processes (Giusti-Suzor 1980) resulted in a powerful method for the evaluation of DR cross sections. It was successfully applied to H_2^+ and its isotopomers (Giusti-Suzor *et al* 1983, Schneider *et al* 1991), O_2^+ (Guberman and Giusti-Suzor 1991, Guberman 2000) and other diatomics, including NO^+ (Sun and Nakamura 1990, Vâlcu *et al* 1998). In the present section, we outline the main ideas and steps of this approach. Although the rotational structure and couplings can now be fully taken into account (Takagi 1993, Schneider *et al* 1997), they are negligible in the case of NO^+ DR (Vâlcu *et al* 1998).

DR involves ionization channels (describing the electron–ion scattering) and dissociation channels (describing the atom–atom scattering). Each ionization channel consists of a Rydberg series of excited states, extrapolated above the continuum threshold, associated with a vibrational level v^+ of the molecular ion. It is *open* if its corresponding threshold is situated *below* the total energy of the system, and *closed* in the opposite case.

In the region of small electron–ion distances, the 'A region' (Jungen and Atabek 1977), the Born–Oppenheimer representation is appropriate to describe the relevant molecular states, and short-range interactions between the ionization and the dissociative channels prevail. In the case of the NO system, they are of Rydberg-valence—or electronic—type (Lefebvre-Brion and Field 1986), and the non-vanishing elements of the interaction matrix $\boldsymbol{\mathcal{V}}$ are given by

$$\boldsymbol{\mathcal{V}}^{\Lambda}_{d_j,lv}(E', E) = \langle \chi^{\Lambda}_{d_j}(R) | V^{\Lambda}_{d_j,l}(R) | \chi^{\Lambda}_{v}(R) \rangle. \tag{2.1}$$

Here E and E' denote the *total* energy of the molecular system, d_j labels one of the dissociative states, l is the orbital quantum number of a partial wave of the external electron and v is the vibrational quantum number, χ^{Λ}_{v} and $\chi^{\Lambda}_{d_j}$ being the vibrational wavefunctions. Being weakly dependent on the energy of the incident electron, $V^{\Lambda}_{d_j,l}(R)$ represents the local coupling between the dissociative state d_j and the *whole* ionization channel associated with lv, and can be

extended to the bound states, below threshold, using the scaling law:

$$V^{\Lambda}_{d_j,l}(R) = v^{\Lambda}_{d_j,nl}(R) \cdot [n - \mu^{\Lambda}_l(R)]^{1.5} \tag{2.2}$$

where $v^{\Lambda}_{d_j,nl}$ is the coupling between the dissociative state d_j and the Rydberg state of principal quantum number n, and $\mu^{\Lambda}_l(R)$ is the quantum defect, also weakly dependent on energy.

Starting from $\boldsymbol{\mathcal{V}}$, one builds the reaction matrix $\boldsymbol{\mathcal{K}}$:

$$\boldsymbol{\mathcal{K}} = \boldsymbol{\mathcal{V}} + \boldsymbol{\mathcal{V}} \frac{\mathbf{1}}{\boldsymbol{E} - \boldsymbol{H}_0} \boldsymbol{\mathcal{K}} \tag{2.3}$$

$\boldsymbol{H}_0$ being the zero-order Hamiltonian associated with the molecular system.

In the external zone, the 'B region' (Jungen and Atabek 1977), represented by large electron–core distances, the Born–Oppenheimer model is no longer valid for the ionization channels and a close-coupling representation in terms of 'molecular ion + electron' is more appropriate. This corresponds to a frame transformation defined by the projection coefficients:

$$\mathcal{C}_{lv^+,\Lambda\alpha} = \sum_v U^{\Lambda}_{lv,\alpha} \langle \chi_{v^+} | \cos(\pi \mu^{\Lambda}_l(R) + \eta^{\Lambda}_{\alpha}) | \chi^{\Lambda}_v \rangle \tag{2.4}$$

$$\mathcal{C}_{d_j,\Lambda\alpha} = U^{\Lambda}_{d_j\alpha} \cos \eta^{\Lambda}_{\alpha}. \tag{2.5}$$

$\mathcal{S}_{lv^+,\Lambda\alpha}$ and $\mathcal{S}_{d_j,\Lambda\alpha}$ are obtained by replacing 'cos' with 'sin' in the above expressions. In the preceding formulae, χ_{v^+} is a vibrational wavefunction of the molecular ion, the index α denotes the eigenchannels built through the *diagonalization* of the reaction matrix $\boldsymbol{\mathcal{K}}$—equation (2.3)—and $U_{lv,\alpha}$ and η^{Λ}_{α} are related to the corresponding eigenvectors and eigenvalues. The projection coefficients shown in (2.4) include the two types of couplings controlling the process: the *electronic* coupling, expressed by the elements of the matrices $\boldsymbol{U}$ and $\boldsymbol{\eta}$, and the *non-adiabatic* coupling between the ionization channels, expressed by the matrix elements involving the quantum defect μ^{Λ}_l. This latter interaction is favoured by the variation of the quantum defect with the internuclear distance R.

The matrices $\boldsymbol{\mathcal{C}}$ and $\boldsymbol{\mathcal{S}}$ with elements (2.4) and (2.5) are the building blocks of the 'generalized' scattering matrix $\boldsymbol{X}$:

$$\boldsymbol{X} = \frac{\boldsymbol{\mathcal{C}} + \mathrm{i}\boldsymbol{\mathcal{S}}}{\boldsymbol{\mathcal{C}} - \mathrm{i}\boldsymbol{\mathcal{S}}} \tag{2.6}$$

whereas the 'proper' scattering matrix, restricted to the *open* channels, is given by (Seaton 1983):

$$\boldsymbol{S} = \boldsymbol{X}_{\mathrm{oo}} - \boldsymbol{X}_{\mathrm{oc}} \frac{1}{\boldsymbol{X}_{\mathrm{cc}} - \exp(-\mathrm{i}2\pi\boldsymbol{\nu})} \boldsymbol{X}_{\mathrm{co}}. \tag{2.7}$$

It is obtained from the sub-matrices $\boldsymbol{X}$ involving the rows and columns associated with the open (o) and closed (c) channels, and a further diagonal matrix $\boldsymbol{\nu}$ formed with the effective quantum numbers $\nu_{v^+} = [2(E_{v^+} - E)]^{-1/2}$ (in au) associated with each vibrational threshold E_{v^+} of the ion situated *above* the current energy E.

For a molecular ion initially in the level v^+_i and recombining with an electron of energy ε, the cross section of capture into *all* the dissociative states d_j of the same symmetry Γ is given by

$$\sigma^{\Gamma}_{\mathrm{diss} \leftarrow v^+_i} = \frac{\pi}{2} \cdot \frac{\rho^{\Gamma}}{2} \cdot \frac{1}{\varepsilon} \cdot \sum_j \sum_l |S^{\Gamma}_{d_j \leftarrow l v^+_i}|^2. \tag{2.8}$$

Here Γ refers to the neutral electronic symmetry ($^2\Sigma^+$, $^2\Pi$ and $^2\Delta$ in this paper) and ρ^{Γ} is the ratio between the multiplicities of the neutral system and the ion. One has to perform the

MQDT calculation for each group of dissociative states of symmetry Γ, and the sum over the resulting cross sections is the total DR cross section:

$$\sigma_{\mathrm{diss}\leftarrow v_i^+} = \sum_{\Gamma} \sigma^{\Gamma}_{\mathrm{diss}\leftarrow v_i^+}. \tag{2.9}$$

3. Molecular data

3.1. Ab initio R-matrix calculations

Up to 1996, the molecular data necessary for the study of the NO^+ DR dynamics over a broad energy range were partial (Raoult 1987) or of questionable consistency (Bardsley 1983, Sun and Nakamura 1990). As an attempt to provide *ab initio* electronic potential curves and couplings between them, Rabadán and Tennyson (1996, 1997) performed a series of fixed geometry R-matrix calculations. The more sophisticated of these calculations (Rabadán and Tennyson 1997, 1998) used the 12 lowest states of NO^+ in a close-coupled expansion. Each of these states was represented using a complete active space valence configuration interaction expansion. Calculations were repeated at 14 internuclear separations from $R = 1.606$ to 2.835 a_0. Calculations at larger values of R, although possibly of significance for this paper, were not attempted because it was found that it was not possible to obtain reliable NO^+ energy levels and wavefunctions at large R with the necessarily limited model employed.

Rabadán and Tennyson computed positions and widths for a number of valence dissociative states, which appear as resonances in the R-matrix scattering calculations, as a function of geometry. Of particular note for this paper are the $A'\ ^2\Sigma^+$, $I\ ^2\Sigma^+$ and $B'\ ^2\Delta$ states, and the three $^2\Pi$ states: $L\ ^2\Pi$, $B\ ^2\Pi$ and $3\ ^2\Pi$. The highly excited $3\ ^2\Pi$ state has never previously been referred to in a DR study.

Although R-matrix calculations of resonance states of a many-electron molecule such as NO have not previously been subjected to detailed calibration against spectroscopic data, such comparisons have been made for Rydberg states of both NO (Rabadán and Tennyson 1997) and CO (Tennyson 1996). These studies both found systematic behaviour in the way the R-matrix calculations represented the bound Rydberg states. As the method is essentially variational, the Rydberg states were, unsurprisingly, found to be uniformly at too high an energy. It was found that the binding energy was underestimated by a constant amount in the quantum defect for a given $n\ell$ series. The error in the quantum defect was about 0.04 for low values of ℓ. The geometry-dependent study on NO also showed that quantum defects, and hence presumably the error in the quantum defects, depend weakly on geometry, except when the curves are perturbed by an avoided crossing. These observations are of importance for the calibration procedure discussed below.

3.2. Calibration of the ab initio data

DR calculations show strong sensitivity to the positions of the neutral curves relative to the ground state of the ion. In particular, a relatively small error in the geometry of curve crossing can lead to a large change in the predicted DR cross section, which is roughly proportional to the square of the nuclear wavefunction overlap from equation (2.1). As discussed above, the R-matrix curves used here can be presumed to be too high relative to the NO^+ ground state and direct use of them yields poor DR cross sections.

We therefore chose to calibrate the *ab initio* curves using data obtained (Raoult 1987) from high-precision spectroscopic measurements (Dressler and Miescher 1981). Our representation of the $NO^+(X\ ^1\Sigma^+)$ state is in good agreement with experimental data, so this curve was taken

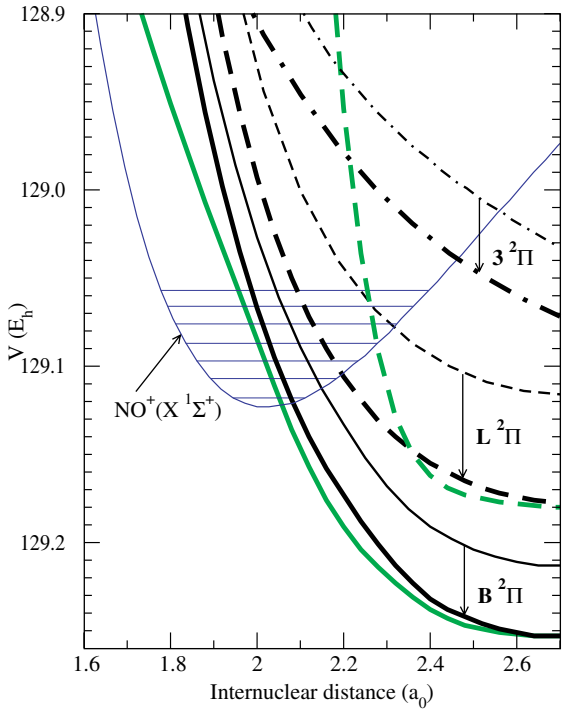

Figure 1. The $^2\Pi$ NO states relevant for the NO^+ DR. Thin black curves: R-matrix results (Rabadán and Tennyson 1997, 1998); thick black curves: translated curves (see text); grey curves: potential curves produced by the MQDT interpretation of spectroscopic data (Raoult 1987). For the ion electronic ground state, the lowest seven vibrational levels are indicated in the figure.

as the benchmark or energy reference when making comparisons. For states of $^2\Pi$ symmetry we calibrated using the MQDT interpretation of the spectroscopic data due to Raoult (1987). A comparison of the *ab initio* data with his curves, see figure 1, is illuminating. The B-state curves have a very similar shape but with the *ab initio* curve displaced to higher energy. As for the L state, the curves are only similar in shape at large R. Indeed, at short internuclear separations, Raoult's curve rises very steeply and crosses the *ab initio* one. As the *ab initio* curve should give an upper bound to the true curve, this suggests that Raoult's curve is less accurate at short R. In fact, there is no available spectroscopic data to characterize the curve in this region. Similarly, there is no data on the 3 $^2\Pi$ state.

To bring the *ab initio* curves into line with the spectroscopic data the following shifts to the *ab initio* curves resulted in what we will refer to below as 'calibrated' curves. Our B $^2\Pi$ potential curve was shifted by -0.04 E$_h$ so that the minima of the calibrated and spectroscopic curves coincide. For $R > 2.9\ a_0$ Raoult's spectroscopic curve was used to define the asymptotic limit. Also, our L $^2\Pi$ potential curve was shifted by -0.06 E$_h$ to bring its minima into agreement with Raoult's curve, and the same curve was used to give the asymptotic limit. The 3 $^2\Pi$ curve was shifted downwards by -0.04 E$_h$. Assuming this as a Rydberg state associated with the B$'$ $^1\Sigma^+$ state of NO^+, this shift corresponds to a change in the quantum defect of approximately 0.04, a figure very much in line with the earlier study of NO Rydberg states (Rabadán and Tennyson 1996, 1997).

Figure 1 illustrates the potential curves of $^2\Pi$ symmetry involved in the above discussion: the *ab initio* potential curves, those produced by MQDT interpretation of spectroscopic data

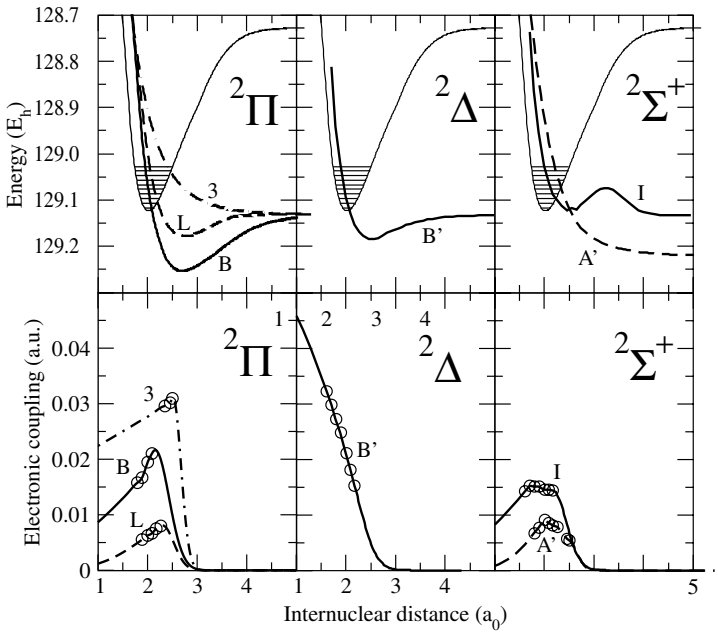

Figure 2. The NO states relevant for the NO^+ DR as a function of total electronic symmetry. Top panels: calibrated potential curves (see text). The ion electronic ground state and the corresponding vibrational levels are represented by thin lines. Bottom panels: couplings between the valence dissociative states and the ionization continua. ○: *R*-matrix data.

(Raoult 1987), and our calibrated curves. It is notable that, while spectroscopic and calibrated B-state curves are similar for all R, the L-state curves differ significantly at short R where the spectroscopic curve is poorly determined.

There is less information available to guide the calibration of the $^2\Delta$ and $^2\Sigma^+$ symmetry curves. The B′ $^2\Delta$ curve was shifted down by -0.06 E_h, in line with the shift of the L $^2\Pi$ state. This shift preserves the curve ordering of Sun and Nakamura (1990). The $^2\Sigma^+$ symmetry curves contain a weakly avoided crossing. We have followed convention by labelling the diabatic curves A′ and I, respectively. The A′ state was shifted down by 0.015 E_h, corresponding to a change in the quantum defect of approximately 0.05 relative to the a $^3\Sigma^+$ parent ion state. The resulting I curve, when extrapolated to its asymptote, has a barrier at $R \sim 3.3\ a_0$, presumably due to a further avoided crossing. This feature has been observed before (Michels 1972). The curves are given in figure 2.

Our calibration of the $^2\Sigma^+$ curves is not well constrained by available data. These curves make essentially no contribution to the DR cross section at low energy and, although they do contribute at higher energies, this contribution is never dominant. Their maximum combined contribution is about 30% of the total cross section near 4 eV.

The *R*-matrix calculations give resonance or autoionization widths as a function of R. Here we have assumed that these widths are the same for the calibrated curves. However, there is no information on the curves or widths outside the range of internuclear distances specified in the *ab initio* calculation. The computed molecular data therefore correspond to a limited, although relevant, range of internuclear distances, and we had to extrapolate the available quantum defects and autoionization widths (leading to the couplings) to the whole range of interest. The curves were extrapolated to large R by connecting them smoothly to

their known dissociation limits. The widths were simply extrapolated in the short R direction and damped to zero at $R = 3\,a_0$ at large R. This behaviour is in agreement with those of the B and L $^2\Pi$ curves modelled by Raoult (1987), but rather arbitrary for the other states. However, our results are almost insensitive to the widths outside the region for which we have actual *ab initio* data.

Figure 2 displays the resulting couplings $V_{d_j}(R)$, related to the widths $\Gamma_{d_j}(R)$ by

$$V^{\Lambda}_{d_j}(R) = [\Gamma^{\Lambda}_{d_j}(R)/(2\pi)]^{1/2} \tag{3.1}$$

together with the corresponding calibrated potential curves for the relevant valence states. It should be noted that previous studies of NO^+ DR (Sun and Nakamura 1990) used somewhat crude estimates of the couplings. In particular, we note that our coupling values for the B$'\,^2\Delta$ state are significantly larger than previously assumed.

4. Evaluation of the cross section using the MQDT-type approach

4.1. Mechanisms and couplings

Using the set of molecular data determined as described above, we performed a series of MQDT calculations of the DR cross section, assuming the molecular ion to be initially in its ground state (X $^1\Sigma^+$, $v_i^+ = 0$). This assumption on the *entrance* (ionization) channel is motivated by our aim to model the most recent storage-ring experiment (Vejby-Christensen *et al* 1998), in which the target ions are cooled to their electronic and vibrational ground state.

The available dissociative channels are the valence states determined by the R-matrix computations. Neglecting spin–orbit effects, we performed three MQDT calculations, each of them involving *simultaneously* all the dissociative states of the same symmetry: one calculation for the states B $^2\Pi$, L $^2\Pi$ and 3 $^2\Pi$, another for I $^2\Sigma^+$ and A$'\,^2\Sigma^+$, and a third one for B$'\,^2\Delta$.

For the energy range of the incident electron, we have explored the interval 0.01 meV–8 eV. Since the dissociation energy of NO^+(X $^1\Sigma^+$) is about 10 eV, part of the 57 vibrational levels of the ion are situated *above* the current total energy of the NO system. These levels are associated with *closed* ionization channels, as defined in section 2, responsible for temporary resonant capture into Rydberg states. As the energy increases, more and more ionization channels become *open*, which can result in autoionization. According to equation (2.7), the interference between the *direct* process (involving open channels exclusively and described by the first term) and the *indirect* one (involving closed channels and accounted for by the second term) results in what we call the *total* process. As shown in figures 3 and 4, the total cross section is characterized by resonance structures, superimposed on a smooth background.

The direct electronic couplings between ionization and dissociation channels—equation (2.1)—have been extracted from the autoionization widths of the valence states. Since a highly accurate solution of the Lippman–Schwinger system of integral equation (2.3) is difficult to obtain (Takagi 1996, 2000, Pichl *et al* 2000), we took advantage of the fact that the couplings involved are small and a perturbative solution is acceptable. As in previous studies (Guberman and Giusti-Suzor 1991, Schneider *et al* 1991) we have adopted the second order of a perturbative expansion, which accounts for all the basic mechanisms involved in DR, including *indirect* electronic interaction between the ionization channels.

The non-adiabatic couplings between the ionization channels rely, see equations (2.4) and (2.5), on the R dependence of quantum defects, which are evaluated using the *ab initio* calculations described in the preceding section. For each dissociative channel available, we have considered its interaction with only one Rydberg series: pπ for the $^2\Pi$ states, pσ for the A$'\,^2\Sigma^+$, sσ for the I$'\,^2\Sigma^+$ and dδ for the B$'\,^2\Delta$ states. Therefore, the 'global' couplings given

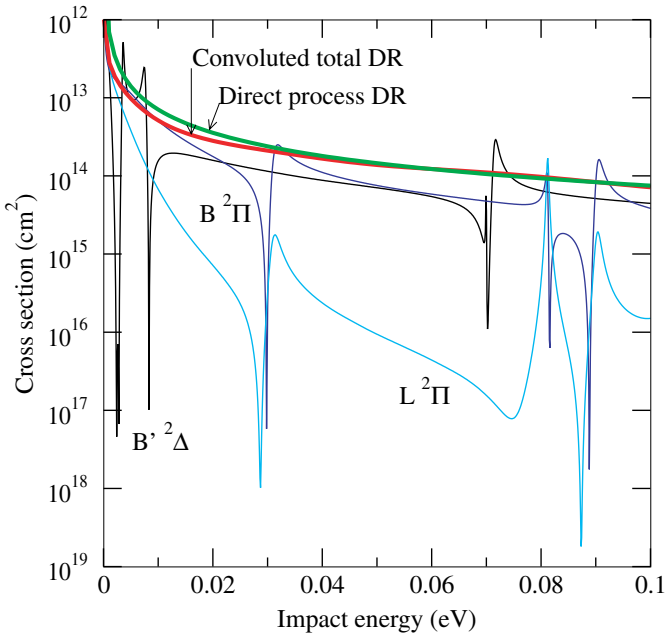

Figure 3. DR cross section of $NO^+(X\ ^1\Sigma^+)$ at low energy. The contribution of the relevant states, according to the present MQDT treatment, is indicated in the figure. The contribution of $3\ ^2\Pi$, $A'\ ^2\Sigma^+$ and $I\ ^2\Sigma^+$ is negligible in this energy range and is not plotted. The 'direct process DR' is the sum of all the *direct* DR cross sections. The 'convoluted total DR' is the sum of all the contributions, convoluted with the anisotropic Maxwell velocity distribution characterizing the ASTRID storage ring ($k_B T_\perp = 20$, $k_B T_\parallel = 1$ meV) (Vejby-Christensen *et al* 1998).

by equation (3.1) are those which have been used as input data for the MQDT computations—$V^{\Lambda}_{d_j,l}(R)$ in equation (2.1).

4.2. The role of the indirect process

The role of the indirect mechanism in the DR process strongly depends on the states and interactions involved. In the case of NO^+ we have found a broad range of situations depending on the symmetry and the nature of the dissociative channel. Even though the indirect process globally plays a minor role for this ion, evaluating its effect gives more insight into the recombination mechanism.

The dominant dissociation paths for the DR of the NO^+ ground state are the $B\ ^2\Pi$ and $B'\ ^2\Delta$ states at low energy (figure 3) and the $3\ ^2\Pi$ state at high energy (figure 4). For these three states, the direct electronic coupling with the entrance ionization channel is relatively strong, of the same order or larger than the coupling with the closed ionization channels. The *average* effect of the indirect process, which manifests itself in the value of the rate coefficients or convoluted cross sections, is small (of the order of 20%) and mostly destructive (see figures 3 and 4).

Conversely, when the direct process is very weak, as is the case for the contribution of the $3\ ^2\Pi$ state at intermediate energy and of the $L\ ^2\Pi$ state at low energy, a significant increase (up to several orders of magnitude) in the cross section is observed when the closed channels, responsible for the indirect mechanism, are included. Figure 5 illustrates this behaviour. This feature has been noted for other molecular ions, H_3^+ (Schneider *et al* 2000, Orel *et al* 2000),

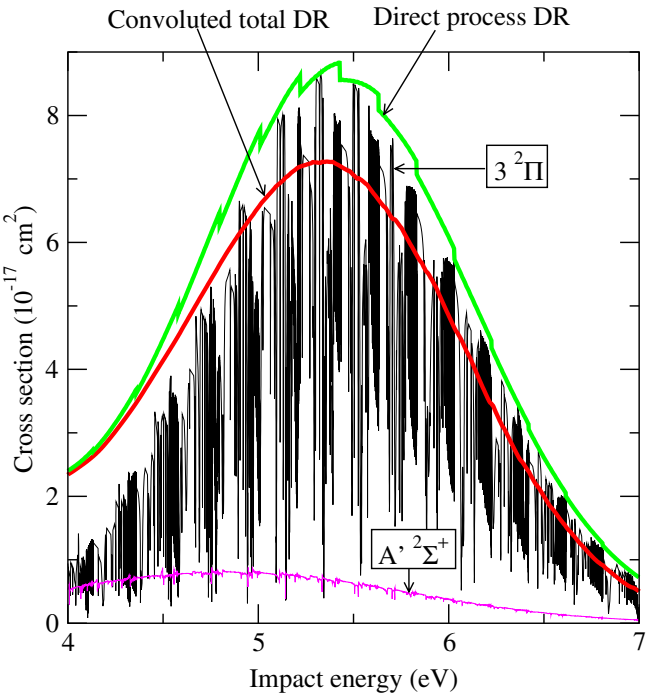

Figure 4. DR of $NO^+(X\ ^1\Sigma^+)$ at high energy. The contribution of the relevant states is indicated in the figure. The contribution of B $^2\Pi$, L $^2\Pi$, B′ $^2\Delta$ and I $^2\Sigma^+$ is negligible in this energy range and is not plotted. The 'direct process DR' is the sum of all the *direct* DR cross sections. The 'convoluted total DR' is obtained as in figure 3.

HeH (Guberman 1994) and O_2^+ (Guberman 2000), at low energy, and relies on a channel mixing effect. The strong interaction between the closed channels associated with high vibrational ion levels and the current dissociative states contaminates, via non-adiabatic or indirect electronic coupling, the direct interaction between the entrance and the dissociative channels, resulting in a strong capture probability.

Due to the presence of much more efficient dissociative routes in each of the energy ranges explored, this feature has no quantitative importance in the present case. However, the phenomenon illustrated in figure 5 is a new example of the spectacular enhancement of the DR probability due to the *closed* channels, which may play a decisive role in the case of very weak direct processes, in particular for the much debated case of H_3^+ (Schneider *et al* 2000, Orel *et al* 2000).

5. Results and discussion

The DR cross sections corresponding to the three symmetries contributing to the process ($^2\Pi$, $^2\Sigma^+$ and $^2\Delta$) were summed according to equation (2.9). In view of the comparison with the storage-ring measurements (Vejby-Christensen *et al* 1998), we have convoluted our MQDT cross sections with the anisotropic Maxwell velocity distribution function for the electrons from the ASTRID device in Aarhus. The transversal and longitudinal temperatures are $k_B T_\perp = 20$ and $k_B T_\parallel = 1$ meV, respectively. The very good agreement with experiment is illustrated in figure 6.

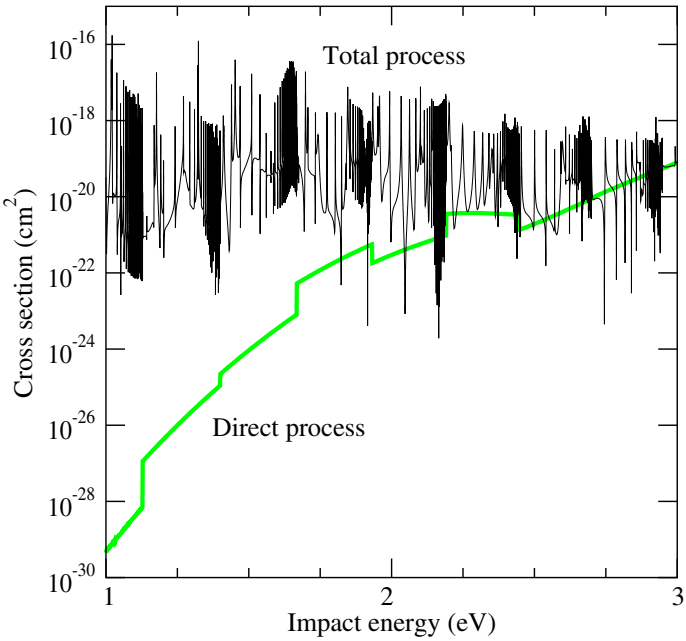

Figure 5. Channel mixing effects in the case of slow direct DR: the capture into the $3\,^2\Pi$ state.

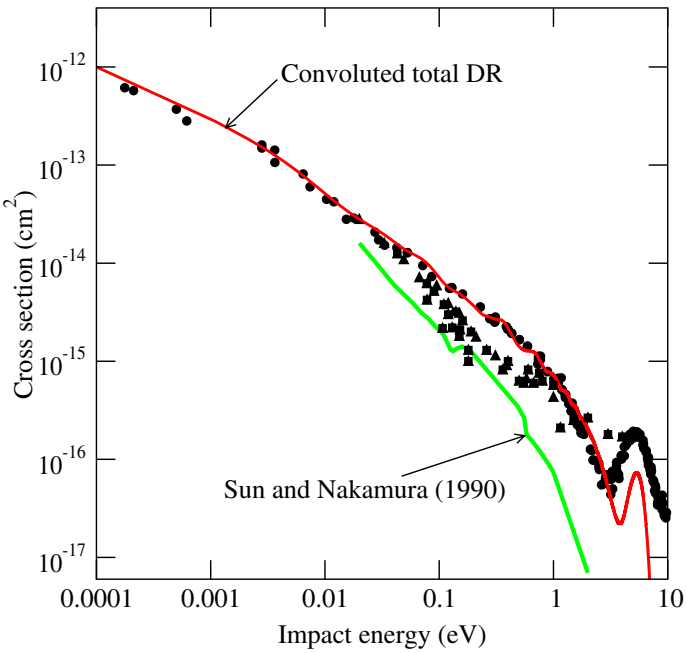

Figure 6. DR of $NO^+(X\,^1\Sigma^+)$. Squares, triangles and circles: experimental cross sections obtained in single-pass (Walls and Dunn 1974, Mul and McGowan 1979) and multipass (Vejby-Christensen *et al* 1998) merged-beam experiments, respectively. 'Convoluted total DR' is the MQDT calculated cross section convoluted as explained in figure 3.

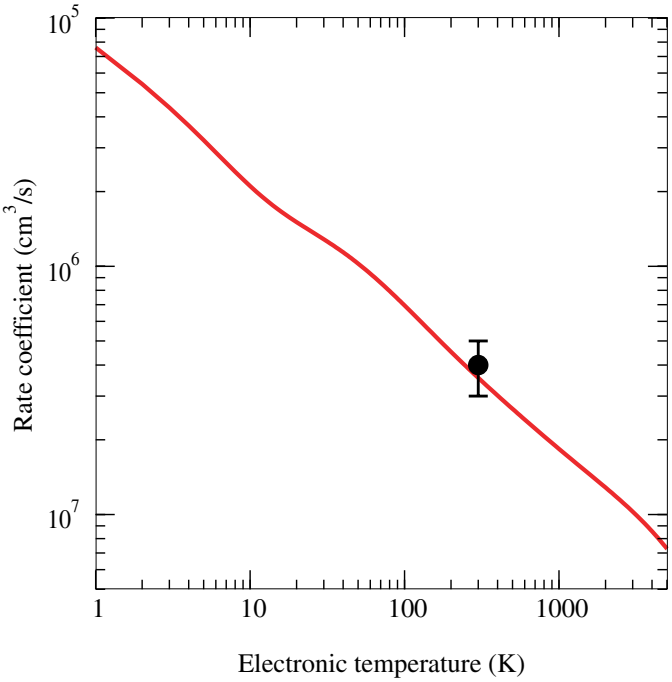

Figure 7. The Maxwell (isotropic) rate coefficient of DR of $NO^+(X\ ^1\Sigma^+)$ as a function of the temperature of the incident electrons. Full curve: present result; ●: thermal (300 K) rate coefficient measured in the most recent experiments (Vejby-Christensen *et al* 1998, Mostefaoui *et al* 1999). The error bars correspond to the data obtained in the plasma measurements (Mostefaoui *et al* 1999).

The role of each dissociation channel depends on the energy of the incident electron. At very low energy, important for the atmospheric and astrophysical environments, B $^2\Pi$, L $^2\Pi$ and B$'$ $^2\Delta$ states dominate the recombination process, as is shown in figure 3. At high energy, the broad peak shown by the ASTRID storage ring is almost entirely due to the 3 $^2\Pi$ state, as shown in figure 4. Our calculations underestimate the size of this peak. There are a number of possible causes for this: the parameters we use for the 3 $^2\Pi$ state have not been calibrated against any spectroscopic data, so must be more uncertain than those of the lower $^2\Pi$ states. Furthermore, above the 3 $^2\Pi$ state there is an increasing number of other resonance states of all symmetries, and it is possible that some or all of these can participate in the DR process via the channel mixing mechanism which is found to be so important for the 3 $^2\Pi$ state.

Starting from the computed cross section, we have evaluated the Maxwell *isotropic* rate coefficient for a broad range of electronic temperatures. The rate is displayed in figure 7, and its thermal (300 K) value is in excellent agreement with the most recent measured values obtained in collision (Vejby-Christensen *et al* 1998) and plasma (Mostefaoui *et al* 1999) experiments.

The contributions of the dissociative channels B $^2\Pi$, L $^2\Pi$, B$'$ $^2\Delta$, I $^2\Sigma^+$ and A$'$ $^2\Sigma^+$ are included in both our theoretical treatment and that of Sun and Nakamura (1990). However the underlying molecular data are different, illustrating once again the sensitivity to these data. Of particular importance at higher energies is the contribution of the 3 $^2\Pi$ state, which is only included in this paper. The improved agreement with experiment at lower energies compared to previous studies (Sun and Nakamura 1990, Vâlcu *et al* 1998) is due mainly to the contribution of the B$'$ $^2\Delta$ state in the present calculations. Its contribution is significant because of the

favourable crossing of its potential curve with that of the ion, but also due to its large coupling to the entrance channel, see figure 2.

6. Conclusions

This paper presents a theoretical study of DR of NO^+ over a broad range of electron energies. Although our basic approach is *ab initio*, using such methods it is not yet possible to compute the positions of the dissociative curves involved in the DR process accurately enough to give reliable results. We have therefore used potential curves derived from spectroscopic data on NO to calibrate the *ab initio* data. Our DR calculations using these calibrated curves give excellent agreement with the low-energy experimental data, up to about 3 eV, significantly improving on previous studies.

A major motivation of this paper was to explain the observed high-energy peak in the cross section at about 5 eV. Our DR calculations give a similar feature when six NO dissociative curves are included. Particularly important for this is the $3\ ^2\Pi$ state which had only been predicted in recent R-matrix studies (Rabadán and Tennyson 1997, 1998) and had therefore been neglected in previous DR calculations. Our calculations do not give quantitative agreement with the observed high-energy peak; it is possible that further curves will be needed to achieve this.

Overall, however, the agreement achieved between theory and experiment over a significant range of energies is very satisfying for the present case of a many-electron target. This suggests that our calibrated *ab initio* approach provides a suitable procedure for studying other many-electron systems for which pure *ab initio* calculations are not reliable.

Acknowledgments

We thank Maurice Raoult for helpful discussions. IFS is grateful to the Royal Society and NATO for a fellowship during which most of this work was completed, as well as to the Institute of Physics and Astronomy at Aarhus and the French CNRS for financial support. Support from the French INSU, British Council, the UK EPSRC, the European Union via the ETR network and the Danish National Research Council through the Aarhus Center for Atomic Physics are also gratefully acknowledged.

References

Andersen L H, Johnson P J, Kella D, Pedersen H B and Vejby-Christensen L 1997 *Phys. Rev.* A **55** 2799
Bardsley J N 1968a *J. Phys. B: At. Mol. Phys.* **1** 349
——1968b *J. Phys. B: At. Mol. Phys.* **1** 365
——1983 *Planet. Space Sci.* **31** 667
Dressler K and Miescher E 1981 *J. Chem. Phys.* **75** 4310
Dulaney J L, Biondi M A and Johnson R 1987 *Phys. Rev.* A **36** 1342
Forck P, Grieser M, Habs D, Lampert A, Repnow P, Schwalm D, Wolf A and Zajfman D 1993 *Phys. Rev. Lett.* **70** 426
Fox J L 1989 *Dissociative Recombination: Theory, Experiment and Applications* vol 4, ed J B A Mitchell and S L Guberman (Singapore: World Scientific) p 264
——1993 *Dissociative Recombination: Theory, Experiment and Applications (NATO ASI Series, Series B: Physics vol 313)* ed B R Rowe, J B A Mitchell and A Canosa (New York: Plenum) p 219
Giusti-Suzor A 1980 *J. Phys. B: At. Mol. Phys.* **13** 3867
Giusti-Suzor A, Bardsley J N and Derkits C 1983 *Phys. Rev.* A **28** 682–91
Greene C H and Jungen C 1985 *Adv. At. Mol. Phys.* **21** 51
Guberman S L 1994 *Phys. Rev.* A **49** R4277

——2000 *Dissociative Recombination: Theory, Experiment and Applications* vol 4, ed M Larsson, J B A Mitchell and I F Schneider (Singapore: World Scientific) p 111
Guberman S L and Giusti-Suzor A 1991 *J. Chem. Phys.* **95** 2602
Jungen C and Atabek O 1977 *J. Chem. Phys.* **66** 5584
Larsson M *et al* 1993 *Phys. Rev. Lett.* **70** 430
Lee C M 1977 *Phys. Rev.* A **16** 109
Lefebvre-Brion H and Field R W 1986 *Perturbations in the Spectra of Diatomic Molecules* (New York: Academic) p 76
Michels H H 1972 *United Aircraft Report* AFWL-TR-72-1
Mostefaoui T, Laubé S, Gautier G, Rebrion-Rowe C, Rowe B R and Mitchell J B A 1999 *J. Phys. B: At. Mol. Opt. Phys.* **32** 5247
Mul P M and McGowan J W 1979 *J. Phys. B: At. Mol. Phys.* **12** 1591
Nakashima K, Nakamura H, Achiba Y and Kimura K 1989 *J. Chem. Phys.* **91** 1603
Orel A E, Schneider I F and Suzor-Weiner A 2000 *Phil. Trans. R. Soc.* A **358** 2445
Pichl L, Nakamura H and Horacek J 2000 *Comput. Phys. Commun.* **124** 1
Rabadán I and Tennyson J 1996 *J. Phys. B: At. Mol. Opt. Phys.* **29** 3747
——1997 *J. Phys. B: At. Mol. Opt. Phys.* **30** 1975
——1998 *J. Phys. B: At. Mol. Opt. Phys.* **31** 4485
Raoult M 1987 *J. Chem. Phys.* **87** 4736
Schmidt H T, Vejby-Christensen L, Pedersen H B, Kella D, Njerre N and Andersen L H 1996 *J. Phys. B: At. Mol. Opt. Phys.* **29** 2485
Schneider I F, Dulieu O and Giusti-Suzor A 1991 *J. Phys. B: At. Mol. Opt. Phys.* **24** L289
Schneider I F, Larsson M, Suzor-Weiner A and Orel A E 2000 *Dissociative Recombination: Theory, Experiment and Applications* vol 4, ed M Larsson, J B A Mitchell and I F Schneider (Singapore: World Scientific) p 131
Schneider I F, Strömholm C, Carata L, Urbain X, Larsson M and Suzor-Weiner A 1997 *J. Phys. B: At. Mol. Opt. Phys.* **30** 2687
Seaton M J 1983 *Rep. Prog. Phys.* **46** 167
Spanel P, Dittrichova L and Smith D 1993 *Int. J. Mass Spectrom. Ion Process.* **129** 183
Strömholm C *et al* 1995 *Phys. Rev.* A **52** R4320
Sun H and Nakamura H 1990 *J. Chem. Phys.* **93** 6491
Takagi H 1993 *J. Phys. B: At. Mol. Opt. Phys.* **26** 4815
——1996 *Dissociative Recombination: Theory, Experiment and Applications* vol 3, ed D Zajfman, J B A Mitchell, D Schwalm and B R Rowe (Singapore: World Scientific) p 174
——2000 *Dissociative Recombination: Theory, Experiment and Applications* vol 4, ed M Larsson, J B A Mitchell and I F Schneider (Singapore: World Scientific) p 180
Tanabe T *et al* 1995 *Phys. Rev. Lett.* **75** 1066
Tanabe T *et al* 2000 *Dissociative Recombination: Theory, Experiment and Applications* vol 4, M Larsson, J B A Mitchell and I F Schneider (Singapore: World Scientific) p 170
Tennyson J 1996 *J. Phys. B: At. Mol. Opt. Phys.* **29** 6185
——2000 *Dissociative Recombination: Theory, Experiment and Applications* vol 4, ed M Larsson, J B A Mitchell and I F Schneider (Singapore: World Scientific) p 121
Vâlcu B, Schneider I F, Raoult M, Strömholm C, Larsson M and Suzor-Weiner A 1998 *Eur. Phys. J.* D **1** 71
Vejby-Christensen L, Kella D, Pedersen H B and Andersen L H 1998 *Phys. Rev.* A **57** 3627
Walls F L and Dunn G H 1974 *J. Geophys. Res.* **79** 1911